Excited State Reservoir Computing using Hybrid Perovskite Electrochemically-Gated Luminescent Cells

Philipp Kollenz[1], Carina Herrle[1], Leonard Göhringer[1], Tom Wickenhäuser[2], Wolfram Pernice[2], Rüdiger Klingeler[2], Felix Deschler[1,*]

[1] Physikalisch-Chemisches Institut, Universität Heidelberg, Im Neuenheimer Feld 229, 69120 Heidelberg

[2] Kirchhoff-Institut für Physik, Universität Heidelberg, Im Neuenheimer Feld 227, 69120 Heidelberg

Abstract

Physical reservoir computing aims to increase computational efficiency of machine learning tasks by shifting the computational burden to a physical system. Reservoirs based on ion dynamics are of particular interest due to the non-linear and integrative nature of ion transport. Here, we demonstrate all-optical operation of a physical reservoir based on electrochemical Li-ion doping of lead halide perovskite microcrystals. Optical excitation changes lithium ion insertion kinetics, which in turn modulate the luminescence response. The heterogenous structure of the crystals leads to a large internal state space of the reservoir. The device can be fabricated using solution-based fabrication and operated using LED illumination, reducing fabrication cost. Our proof-of-concept results demonstrate optically excited state dynamics and ion transport as a promising platform for physical reservoir computing.

Introduction

The continued scaling and deployment of AI systems faces critical challenges related to energy consumption, hardware complexity, and the sheer volume of data required to train and operate modern algorithms. Underlying many of these issues are the fundamental constraints imposed by traditional computing architectures. Conventional von Neumann systems, with their clear separation of memory and processing units, are approaching intrinsic performance limits, prompting the search for paradigms that can transcend these barriers.

One promising avenue is neuromorphic computing, which seeks to mimic the brain's structure and operational principles, such as the leaky integrate-and fire behavior of spiking neural networks.[1] Hybrid digital-analog platforms such as BrainScaleS[2] hold the potential for substantial gains in energy efficiency and adaptability. However, many candidate neuromorphic systems face challenges regarding their trainability compared to conventional gradient-based learning methods.

Within this landscape, physical reservoir computing (PRC) has emerged as a compelling concept that leverages the natural dynamics of physical systems as a computational resource. Reservoir computing shifts the focus away from training every node in a network, instead exploiting inherent nonlinearities, connections, and temporal dependencies present in suitable physical media, to transform the input data into a high-dimensional internal state space. The state of this system can be interpreted using a simple classical machine learning model, greatly reducing training cost. Such strategies draw inspiration from biological systems, where groups of neurons act as reservoirs to increase adaptability on new tasks.[3]

For PRC to serve as a practical alternative, it must meet key criteria: low energy consumption, repeatable nonlinear responses, coupled internal states, and a capacity to encode temporal information. Ion transport dynamics which are central in biological systems fulfill many of these criteria: Just as ions in living cells modulate membrane potentials and synaptic states, ion-gated reservoirs can exploit electrochemical phenomena to create tunable, time-dependent dynamical behavior that inherently process and transform input signals.[4] However, the speed of data throughput is limited by the diffusion of ions trough the material.[5]

Recently, a different approach using optically excited charge carriers instead of ions was repoted.[6] In these "memlumors", input data is written into the system by a pump laser, and the response is read out through the photoluminescence of the material. This photoexcited mechanism can yield highly nonlinear, energy-efficient, and fast response dynamics. Since the excitation and emission are managed optically, no contacts and therefore no complex microstructures are required.

Our approach combines the strengths of ion-based reservoir computing and optically excited carrier dynamics inside a heterogenous perovskite thin film. By adjusting the optical excitation intensity, we can influence ion transport[7, 8], which in turn modifies luminescence and excitation absorption within the reservoir. Remarkably, this hybrid strategy can be implemented with simple, low-cost equipment: our system can be pumped using an LED, and the output can be read out with commercial CMOS sensors. Furthermore, the heterogenous structure of the material forms on its own during scalable solution processing, reducing fabrication complexity. The used read-out areas in the range of 100 um translate to 10^4 nodes per cm². This fusion of ion-based and optically excited dynamics leverages the intrinsic nonlinearities, efficiency and temporal memory of ion-gated reservoirs, while simultaneously allowing for faster and contactless data throughput.

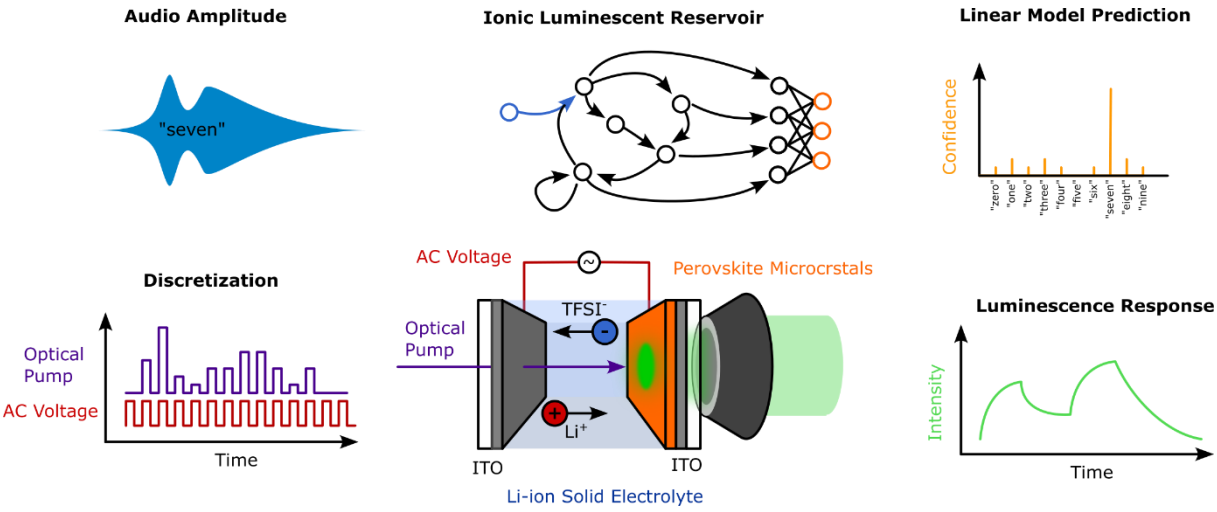

Figure 1: General scheme for opto-ionic reservoir computing: Time-series data such as spoken digit audio waveforms are converted into optical excitation pulses synchronized with an AC voltage. The heterogenous and time-dependent nature of the physical reservoir transforms the input data into a higher-dimensional state space. This space is read out using photoluminescence microscopy and interpreted using a linear regression model.

Results

Photoexcited States in Ion-Gated Hybrid Perovskite as an Opto-ionic Reservoir

Our reservoir material consists of a polycrystalline layer of MAPbBr3 microcrystals on ITO-coated glass. Lithium ions are supplied from a film of solid electrolyte consisting of LiTFSI and polyethylene oxide, using aluminum as a counter electrode. Application of a voltage across the device causes insertion/removal of the ions into the perovskite crystals, modulating the photoluminescence response. Optical excitation using LED light in turn alters the ion insertion kinetics, which influences the photoluminescence response. The PL response serves as readout from the reservoir after evolution of the initial excited state population by diffusion and recombination.

This behavior is exploited to write data into the reservoir by using phase-modulated optical excitation pulses synchronized to an applied AC voltage. (Fig. 2A) If the optical excitation is in phase with the applied voltage, the photoluminescence intensity decreases as a result of excess Li insertion into the perovskite. In contrast, out-of-phase excitation causes an increase in photoluminescence due to the increased removal of Li-ions. (Fig. 2B) This is likely the result of increased ion conductivity upon photoexcitation: Photoexcited charge carriers can screen the effect of charged point defects which otherwise would slow down ions. Furthermore, photoexcitation can lead to phase transitions which result in weaker bonds and therefore a softer material, facilitating ion transport.[9]

The perovskite film consists of many crystallites with varying shapes and sizes. Since ion insertion only occurs at the interface between electrolyte and perovskite, the insertion rate and therefore optical response is dependent on the size and aspect ratio of the crystals. This can be seen by the variation in kinetics at different positions on the photoluminescence microscopy image. (Fig. 2C) To quantify these differences, the PL microscopy video is decomposed into a linear combination of time-invariant images and their time-dependent weights using principal component analysis (PCA). Figure 2E shows the first four components of this decomposition. While the first two components mainly cover large-scale changes in the PL intensity caused by larger crystals, components 3 and 4 focus more on smaller features. This demonstrates a higher-dimensional internal state space of the system, which is a requirement for reservoir computing. Plotting the time-dependent components against each other reveals hysteresis loops. (Fig. 2F) This indicates that the state of the system at a specific point in time is dependent on its history, which is another important property of reservoir systems.

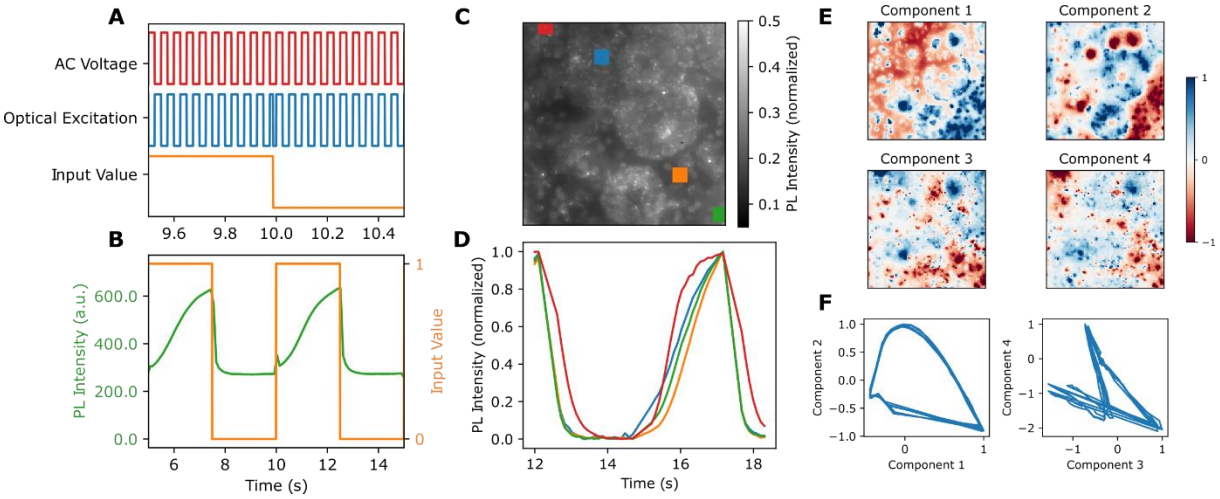

Figure 2: Opto-ionic response used for physical reservoir computing: **A:** Binary data is written into the reservoir by an AC voltage and synchronized pulses of light. **B:** Modulation of the binary input causes changes in PL intensity which are integrative and non-linear. **C, D:** PL microscopy shows the inhomogeneities of the microcrystal film, which causes a range of time-dependent luminescence responses. **E:** Decomposition of the spatially varying kinetics using principal component analysis. **F:** Amplitude of the components during cycling shows hysteresis loops, demonstrating internal memory of the system.

Electro-optic modulation of excited state dynamics by lithium insertion

To demonstrate the impact of lithium insertion on the optical properties of the material, constant current of +/- 40 nA is applied to the cell for 5 minutes each cycle. Assuming 100% faradic efficiency, the resulting charge would correspond to an inserted Li-ion density of $7x10^{-18}$ cm^{-3} or $5x10^{-4}$ per $MAPbBr_3$ unit cell, comparable to the doping concentration achieved by Mathieson et al. in thicker $MAPbBr_3$ samples using the same electrolyte.[10]

Time-correlated single photon counting (TCSPC) measurements at different stages of the insertion reveal a decrease in photoluminescence intensity and increase in short-timescale recombination upon Li insertion. (Fig. 2C) Steady-state photoluminescence spectra show a shift in emission peak wavelength by 5 nm as well as a reduction in peak intensity by a factor of 10 between the fully inserted and removed states.

A possible mechanism for these charging-induced optical changes is the Insertion of lithium into the crystal structure. Inserted Li-ions cause defects, which allows for an increase in non-radiative recombination of excited state charge carriers, leading to a decrease in photoluminescence lifetime and intensity. Based on diffusion and bimolecular recombination kinetics, the resulting charge carrier density under optical excitation will be show a non-linear response to the ion concentration modulation. The shift in photoluminescence emission wavelength can be attributed to donating of electrons from the inserted lithium into the conduction band of the perovskite, increasing the bandgap.[11] During charging, the lithium ions also form an electric double layer at the perovskite-electrolyte interface, causing a strong electric field at the crystal surface. This may cause screening effects which further alter recombination kinetics and bandgap.[12] As these two effects (lithium insertion and double layer field effect) scale differently in respect to the crystal thickness, this further increases the spatial heterogeneity in excited state and Li insertion dynamics in our polycrystalline samples, widening the reservoir state dimension space.

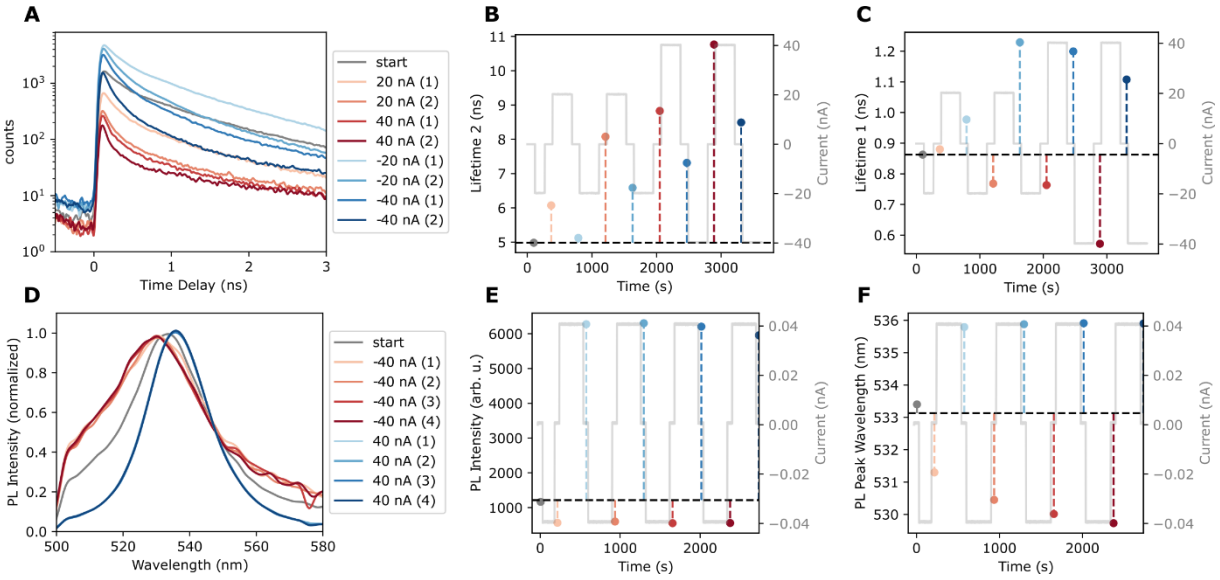

Figure 3: Influence of Lithium insertion/removal on the photoluminescence signal. **A**: Operando TCSPC traces at different stages of the lithium insertion/removal process. **B, C:** Resulting lifetimes of a biexponential fit **D:** Static PL spectrum at different stages of the insertion/removal process **E, F:** Peak intensity and wavelength of a Lorentzian fit of the spectrum.

Exploiting Microstructure to increase Reservoir State Complexity

The main purpose of physical reservoirs is to transform input data into a higher-dimensional latent space, facilitating data processing by classical computationally-cheap machine learning methods. The size of this space was explored by writing integers up to 4-bit into the system using in-phase (digital 1) or out-of-phase (digital 0) light pulses with respect to the applied AC voltage. (Fig. 4A) After each writing sequence, the state of the system was read out by (spectrally averaged) photoluminescence microscopy over an area of 100um. The system was then returned to its initial state by applying a long positive, negative and then neutral voltage, erasing its memory. (Fig. 4B) This is repeated 20 times for each bit sequence. The resulting PL intensity microscopy images were then decomposed into linear combinations of sequence-independent spatial maps and their spatially-independent weights using PCA. The spatial maps of the first four principal components are shown in Fig. 4C, highlighting the difference in PL response between crystals. The corresponding weights to the principal components assign each sequence to a point in a 4-dimensional state space of the reservoir. To better visualize this space, the points are projected into two dimensions using t-distributed stochastic neighbor embedding (t-SNE). Figure 4D shows that data points with the same input sequence naturally form clusters, which can be distinguished already by eye, indicating that the reservoir state space has memory depth of at least 4 bits.

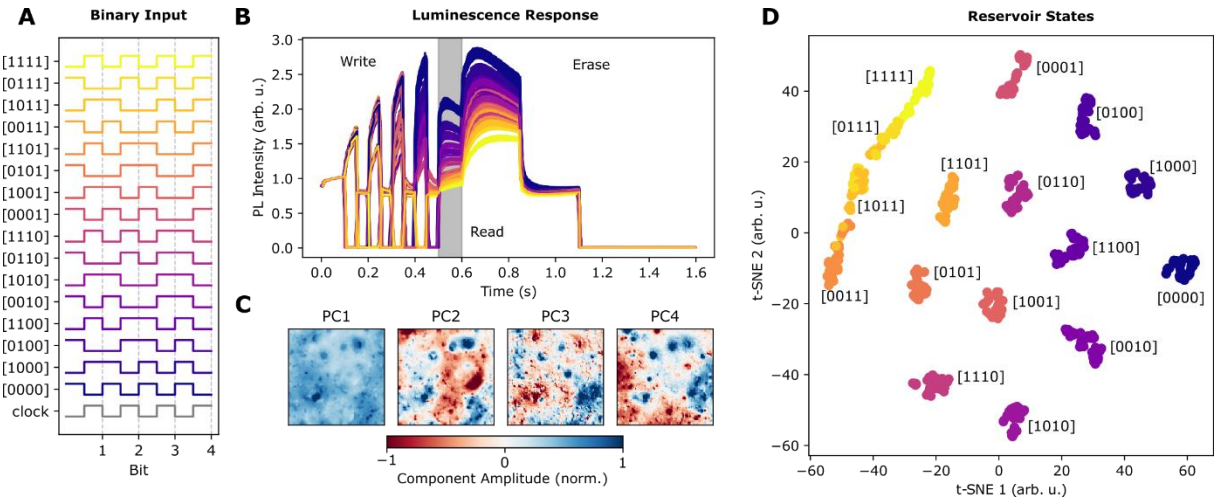

Figure 4: Application of the reservoir to a 4-bit memory task: **A:** Encoding of a 4-bit integer into in/out-of-phase optical excitation pulses against the applied AC voltage. **B**: Spatially averaged PL response of the reservoir to input of different integers. A higher integer value generally corresponds to a higher PL intensity at readout. **C**: Decomposition of the spatial inhomogeneities into four principal components. **D**: 4D principal component space of the reservoir visualized by t-SNE dimensionality reduction. The Reservoir states for each integer can be easily identified.

Conclusions

The excited state populations in heterogenous thin films of Li-doped hybrid perovskite are capable to perform opto-ionic reservoir computing. The luminescent response of the material can be controlled optically by timed pulses of LED light synchronized to a low AC voltage. This is mediated by light-sensitive insertion or removal of lithium ions into the perovskite, causing heterogenous changes in excited state recombination kinetics. This behavior is exploited to encode up to four bits of binary data, resulting in a multidimensional reservoir state space that can be probed using photoluminescence microscopy. At a frequency of 20 Hz and a node density of 10^4 cm^{-2}, this results in an energy consumption of 500 nJ per operation, which arises from the current continuous nature of illumination and electrical driving. As the data access is all-optical, the node density and writing speed could be further optimized down to the diffraction limit of visible light. Using patterned light, this would lead to node densities of 10^9 cm^{-2} and energy consumption of 2 fJ per operation, assuming an optimized writing speed of 2 kHz. This serves as a proof of concept for time-series data processing using luminescent opto-ionic reservoirs. As the system is simple to fabricate and can be driven using standard electronics, this opens up new routes for low-cost neuromorphic hardware development.

Methods

Methylammonium Lead Tribromide Microcrystal Thin Films

Under Nitrogen atmosphere, MABr and PbBr2 were dissolved in DMF at room temperature. ITO-coated glass (1.1mm, 30 Ohm/sq) was cut into 16x16mm squares and activated using ozone treatment. The solution was spin-coated on the substrates at 1600 rpm for 20s. The resulting thin films were annealed for 15min at 80°C. The films were stored under nitrogen atmosphere for up to one month.

Polymer Solid Electrolyte Films

Polyethylene oxide (600k, Sigma-Aldrich) and LiTFSI was dissolved in Acetonitrile and stirred at 60°C for 2h. The solution was blade-coated on 20x5mm Aluminium foil sheets (15um) at a wet thickness of 1mm. The films were dried at room temperature for 1h and at 60°C for 1h, resulting in a dry film thickness of 100 um. The films were stored at a temperature of 21°C and relative humidity of 40% for up to one month.

Assembly of the Hybrid Perovskite Reservoir Electrochemical Cell

Polymer solid electrolyte films were pressed onto the perovskite thin films at 2 kPa for 20 s. At the edges, the perovskite was removed using Acetone. The aluminium and ITO current collectors were contacted using copper tape. Any unwanted contact between the aluminium and ITO current collectors was isolated using clear adhesive tape. The device was encapsulated using clear adhesive tape. The resulting cells were stored for up to 24h before the experiment.

Operando Photoluminescence Spectroscopy/Microscopy

An Olympus BX61 upright epifluorescence microscope was modified to incorporate a fiber-coupled 430nm LED (Thorlabs) as an excitation light source. A 100 mm Achromatic doublet was used to focus the excitation light into the back focal plane of the 20x NA = 0.4 objective. A 500 nm dichroic mirror as well as 450 nm short- and longpass filters were used to separate the optical excitation from the photoluminescence signal. Either a CMOS camera (Basler Ace acA720-520um) or a fiber-coupled spectrometer (OceanOptics HDX-VIS) were used to detect spatial or spectral variations in the photoluminescence response. All measurements were performed at an intensity of 300 mW/cm^2. The voltage and current across the cell was controlled using a BioLogic SP200 potentiostat with ultra-low current (ULC) probe.

Operando TCSPC Experiment

Ultrafast excitation pulses at 400 nm were generated by second harmonic generation in BBO from a mode-locked Ti:Sapph laser (Coherent Mira, 100 fs, 800 nm, 80 MHz). The excitation was directed at the sample using a 75 mm plano-convex lens, resulting in a fluence of 30 nJ/cm^2. The resulting emission was captured using a 50 mm plano-convex lens and a

monochromator was used to select the emission peak at 530 nm. Time traces were captured for 10s during the Li insertion/removal process. The voltage and current across the cell were controlled using a BioLogic SP200 potentiostat with ultra-low current (ULC) probe.

References

[1] W. Maass, *Neural Networks* **1997**, *10*, 1659-1671.

[2] C. Pehle, S. Billaudelle, B. Cramer, J. Kaiser, K. Schreiber, Y. Stradmann, J. Weis, A. Leibfried, E. Müller, J. Schemmel, *Frontiers in Neuroscience* **2022**, *16*.

[3] P. Enel, E. Procyk, R. Quilodran, P. F. Dominey, *PLOS Computational Biology* **2016**, *12*, e1004967.

[4] K. Shibata, D. Nishioka, W. Namiki, T. Tsuchiya, T. Higuchi, K. Terabe, *Scientific Reports* **2023**, *13*, 21060.

[5] A. Sood, A. D. Poletayev, D. A. Cogswell, P. M. Csernica, J. T. Mefford, D. Fraggedakis, M. F. Toney, A. M. Lindenberg, M. Z. Bazant, W. C. Chueh, *Nature Reviews Materials* **2021**, *6*, 847-867.

[6] A. Marunchenko, J. Kumar, A. Kiligaridis, D. Tatarinov, A. Pushkarev, Y. Vaynzof, I. G. Scheblykin, *ACS Energy Letters* **2024**, *9*, 2075-2082.

[7] A. Senocrate, E. Kotomin, J. Maier, *Helvetica Chimica Acta* **2020**, *103*, e2000073.

[8] D. W. deQuilettes, W. Zhang, V. M. Burlakov, D. J. Graham, T. Leijtens, A. Osherov, V. Bulović, H. J. Snaith, D. S. Ginger, S. D. Stranks, *Nature Communications* **2016**, *7*, 11683.

[9] Y.-C. Zhao, W.-K. Zhou, X. Zhou, K.-H. Liu, D.-P. Yu, Q. Zhao, *Light: Science & Applications* **2017**, *6*, e16243-e16243.

[10] A. Mathieson, S. Feldmann, M. De Volder, *JACS Au* **2022**, *2*, 1313-1317.

[11] A. G. M. Mathieson, W. M. Dose, H.-G. Steinrück, C. J. Takacs, S. Feldmann, R. Pandya, A. J. Merryweather, D. Mackanic, A. Rao, F. Deschler, M. De Volder, *Energy & Environmental Science* **2022**, *15*, 4323-4337.

[12] H. T. Yi, S. Rangan, B. Tang, C. D. Frisbie, R. A. Bartynski, Y. N. Gartstein, V. Podzorov, *Materials Today* **2019**, *28*, 31-39.